Rare hadronic charged B meson decays at LHCb

Tom Hadavizadeh

St Peter's College

University of Oxford

A thesis submitted for the degree of

Doctor of Philosophy

Trinity 2018

Contents

List of Figures

List of Tables

Chapter 1

Introduction

Contents

1.1 Something

Here's a thing I did [1].

Chapter 2

Theory

Contents

2.1 The Standard model of Particle of Physics

2.2 Annihilation topology decays

2.2.1 Other annihlation decays

2.3 Theoretical predictions for $B^+ \to D_s^+ \phi$ decay

2.3.1 Standard model predictions

2.3.2 BSM models and predictions

2.3.3 Previous measurements

2.4 Theoretical predictions for $B^+ \to D_s^+ K^+ K^-$ decay

2.4.1 Standard model predictions

2.4.2 Previous measurements

Chapter 3

The LHCb detector

Contents

3.1 The LHC

3.1.1 Overview

3.1.2 The accelerator complex

3.1.3 Beam conditions at LHCb

3.2 The LHCb experiment

3.2.1 Trackers

3.2.2 Ring imaging Cherenkov detectors

3.2.3 Calorimeters

3.2.4 Muons

3.2.5 Trigger

Chapter 4

Event selection

Contents

In this chapter the procedure developed to reconstruct and select $B^+ \to D_s^+\phi$ and $B^+ \to D_s^+K^+K^-$ candidates is described. In both cases the branching fractions are measured relative to the normalisation channel $B^+ \to D_s^+\overline{D}^0$. The corresponding selection for the normalisation channel $B^+ \to D_s^+\overline{D}^0$ is also described.

4.1 Dataset

The search for $B^+ \to D_s^+\phi$ and $B^+ \to D_s^+K^+K^-$ decays are both performed using data taken

Table 4.1: The integrated luminosities obtained during the different data taking periods used in this analysis and the corresponding centre-of-mass energies ($\sqrt{s}$).

Year	Integrated luminosity (fb^{-1})	$\sqrt{s}$ (TeV)
2011	1.0	7
2012	2.0	8
2015	0.3	13
2016	1.5	13

Data taken with the LHCb experiment in Run 1 (2011 and 2012) and part of Run 2 (2015 and 2016) are used in this analysis. The total integrated luminosity obtained for each year of data taking is listed in Table 4.1, along with the corresponding centre-of-mass energies.

4.2 Online selection

The online event selection is performed by the LHCb trigger, which consists of a hardware stage, based on information from the calorimeter and muon systems, followed by a software stage, which reconstructs the full event. Reconstructed objects are classified into categories when considering their relationship to the various triggers that fired in a given event.

- If the interaction caused by a reconstructed object was sufficient to have fired a given trigger then this object is said to be `TOS` (Triggered on Signal) with respect to that trigger. As such, if the hits that this object caused were removed from the events the trigger would no longer fire.

- Conversely, if the object did not cause the trigger to have fired, the object is `TIS` (Triggered Independently of Signal) with respect to the trigger. In this case, removal of any hits from the object would not affect the trigger decision.

- A third category is possible, `TOB` (Triggered on Both), where both the signal object and another object are required to reach the threshold to fire a trigger. In this situation neither are sufficient to individually fire the trigger, but removing

either one of them would prevent the trigger firing. Events in this category are not considered in this analysis.

At the hardware trigger stage, the selected candidates are required to be `TOS` with respect to the hadronic trigger `L0Hadron`. This ensures the selected candidates were retained due to corresponding deposits in the hadronic calorimeter. Alternatively, candidates are selected if they are `TIS` with respect to the global hardware trigger `L0Global`. This allows candidates that have been retained due another highly energetic decay in the same event to contribute. This could be the decay of hadron resulting from the other b quark in a $b\bar{b}$ pair production. Any of the hardware trigger subsystems can contribute to the `L0Global` decision.

- Include approximate TIS TOS fractions

The software trigger stage is split into two parts, HLT1 and HLT2. The first stage HLT1 requires that the the selected candidates are associated with well reconstructed tracks.

At the second software stage, HLT2, two different algorithms are used to select candidates for this analysis. The first one uses a multivariate algorithm [2] to identify the presence of a secondary vertex that has two, three or four tracks and is displaced from any PV. At least one of these charged particles must have a transverse momentum $p_{\mathrm{T}} > 1.7\,\mathrm{GeV}/c$ and be inconsistent with originating from a PV. The second algorithm selects ϕ candidates decaying to two charged kaons. Each kaon must have a transverse momentum $p_{\mathrm{T}} > 0.8\,\mathrm{GeV}/c$ and be inconsistent with originating from a PV. The invariant mass of the kaon pair must be within $20\,\mathrm{MeV}/c^2$ of the known ϕ mass [3]. The inclusive ϕ line is used to maximise the selection efficiencies

- fractions of events added by each category

4.3 Offline selection

Events passing any trigger requirement are saved to tape for processing offline. The stages of this offline reconstruction are detailed in this section.

4.3.1 Selection requirements

The large offline data samples passing the online trigger selection are habitually processed in a procedure know within LHCb as *Stripping*. This centrally managed processing builds candidates from tracks and neutral calorimeter objects in each event according to a set of predefined *Stripping Lines*. Each line builds a specific candidate decay, applying a loose set of preselection requirements, including kinematic, geometric and invariant mass selections.

The candidate $B^+ \to D_s^+\phi$ and $B^+ \to D_s^+K^+K^-$ decays are built using a very similar set of requirements due to the similar topologies of these decays. The normalisation channel, $B^+ \to D_s^+\overline{D}^0$ is built similarly, however the difference in lifetime between the $\overline{D}^0$ and ϕ mesons necessitates a slightly different topology. The fully hadronic final state means that candidates are built from the combination of five tracks. Only *long* tracks (those with hits in the VELO and tracking stations) are used to build these mesons. To ensure these are well reconstructed, the track χ^2 per degree of freedom is required to be below 4.0. Additionally they are required to have a total momentum $p > 1000\,\text{MeV}/c$ and momentum transverse to the beam direction of $p_\text{T} > 100\,\text{MeV}/c$.

- Track selection
- D_s^+ and ϕ construction
- B^+ construction
- diagram of topologies
-

The searches for $B^+ \to D_s^+\phi$ and $B^+ \to D_s^+K^+K^-$ decays employ the use of two different *Stripping Lines* as detailed in Table 4.2. These differ only in the invariant mass window applied to the K^+K^- pair used to reconstruct the ϕ meson, and in the number of D_s^+ decay modes included: the $B^+ \to D_s^+K^+K^-$ line only reconstructs the

Table 4.2: Stripping lines used in this analysis.

Mode	Stripping line
$B^+ \to D_s^+ \phi$	`StrippingB2DPhiD2HHHPIDBeauty2CharmLine`
$B^+ \to D_s^+ K^+ K^-$	`StrippingB2DKKD2HHHCFPIDBeauty2CharmLine`
$B^+ \to D_s^+ \overline{D}^0$	`StrippingB2D0DBeauty2CharmLine`

Cabibbo Favoured (CF) $D_s^+ \to K^+ K^- \pi^+$ decay. The *Stripping Line* used to select the normalisation channel $B^+ \to D_s^+ \overline{D}^0$ is also included in Table 4.2. This has slightly different requirements allowing the $\overline{D}^0$ meson decay vertex to be be displaced from the B^+ meson decay vertex.

The selection requirements imposed on candidate $B^+ \to D_s^+ \phi$ and $B^+ \to D_s^+ K^+ K^-$ decays in their respective *Stripping Lines* is detailed in Table 4.3.

Two slightly different strategies are used for the normalisation channel selection in the search for $B^+ \to D_s^+ \phi$ and $B^+ \to D_s^+ K^+ K^-$ events. In the former, the dedicated $B^+ \to D_s^+ \overline{D}^0$ stripping line listed in Table 4.2 is used to reconstruct the normalisation channel decays. The Stripping Line selection for this line is listed in Table 4.4.

The Stripping Line used in the search for $B^+ \to D_s^+ K^+ K^-$ decays covers the full $m(K^+ K^-)$ phasespace. This includes the $\overline{D}^0$ mass such that this line reconstructs both the signal and normalisation channels simultaneously. Both modes are selected using this line to reduce systematic uncertainty in the ratio of selection efficiencies.

Table 4.3: Selection requirements for $B^+ \to D_s^+\phi$ and $B^+ \to D_s^+K^+K^-$ candidates.

Particles	Quantity	Requirement
B^+	Mass	$4750 < m(D_s^+\phi) < 7000\,\mathrm{MeV}/c^2$
	Products p_T scalar sum	$\sum p_\mathrm{T} > 5000\,\mathrm{MeV}/c$
	Vertex quality	$\chi^2/N_\mathrm{DOF} < 10$
	Lifetime	$\tau_{B^+} > 0.2\,\mathrm{ps}$
	Impact parameter significance	$\chi^2_\mathrm{IP} < 25$
	Direction angle	$\cos\theta > 0.999$
	>0 decay products with:	
	Momentum	$p > 10000\,\mathrm{MeV}/c$
	Transverse momentum	$p_\mathrm{T} > 1700\,\mathrm{MeV}/c$
	Impact parameter significance	$\chi^2_\mathrm{IP} > 16$
	Impact parameter	$\mathrm{IP} > 0.1\,\mathrm{mm}$
	>1 decay products with:	
	Momentum	$p > 5000\,\mathrm{MeV}/c$
	Transverse momentum	$p_\mathrm{T} > 500\,\mathrm{MeV}/c$
D_s^+	Mass	$1770 < m(h^+h^-h^+) < 2068\,\mathrm{MeV}/c^2$
	Products p_T scalar sum	$\sum p_\mathrm{T} > 1800\,\mathrm{MeV}/c$
	Distance of closest approach	$\mathrm{DOCA}(h^+, h^-) < 0.5\,\mathrm{mm}$
	Distance of closest approach	$\mathrm{DOCA}(h^+, h^+) < 0.5\,\mathrm{mm}$
	Direction angle	$\cos\theta > 0$
	Vertex quality	$\chi^2/N_\mathrm{DOF} < 10$
	Flight distance significance	$\chi^2_\mathrm{FD} > 36$
ϕ	Mass (only for $B^+ \to D_s^+\phi$)	$\lvert m(K^+K^-) - m_\phi\rvert < 150\,\mathrm{MeV}/c^2$
	Distance of closest approach	$\mathrm{DOCA}(K^+, K^-) < 0.5\,\mathrm{mm}$
	Direction angle	$\cos\theta > 0$
	Vertex quality	$\chi^2/N_\mathrm{DOF} < 16$
	Flight distance significance	$\chi^2_\mathrm{FD} > 16$
K^+ (π^+)	Track quality	$\chi^2/N_\mathrm{DOF} < 4.0$
	Transverse momentum	$p_\mathrm{T} > 100\,\mathrm{MeV}/c$
	Momentum	$p > 1000\,\mathrm{MeV}/c$
	Impact parameter significance	$\chi^2_\mathrm{IP} > 4$
	Ghost track probability	$P_\mathrm{Ghost} < 0.4$
	Particle identification	$\mathrm{PIDK} < 20$ ($\mathrm{PIDK} > -10$)

Table 4.4: Selection requirements for $B^+ \to D_s^+ \overline{D}^0$ candidates.

Particles	Quantity	Requirement
B^+	Mass	$4750 < m(D_s^+ \overline{D}^0) < 7000\,\text{MeV}/c^2$
	Products p_T scalar sum	$\sum p_\text{T} > 5000\,\text{MeV}/c$
	Vertex quality	$\chi^2/N_\text{DOF} < 10$
	Lifetime	$\tau_{B^+} > 0.2\,\text{ps}$
	Impact parameter significance	$\chi^2_\text{IP} < 25$
	Direction angle	$\cos\theta > 0.999$
	>0 decay products with:	
	Momentum	$p > 10000\,\text{MeV}/c$
	Transverse momentum	$p_\text{T} > 1700\,\text{MeV}/c$
	Impact parameter significance	$\chi^2_\text{IP} > 16$
	Impact parameter	$\text{IP} > 0.1\,\text{mm}$
	>1 decay products with:	
	Momentum	$p > 5000\,\text{MeV}/c$
	Transverse momentum	$p_\text{T} > 500\,\text{MeV}/c$
D_s^+	Mass	$1770 < m(h^+h^-h^+) < 2068\,\text{MeV}/c^2$
	Products p_T scalar sum	$\sum p_\text{T} > 1800\,\text{MeV}/c$
	Distance of closest approach	$\text{DOCA}(h^+, h^-) < 0.5\,\text{mm}$
	Distance of closest approach	$\text{DOCA}(h^+, h^+) < 0.5\,\text{mm}$
	Direction angle	$\cos\theta > 0$
	Vertex quality	$\chi^2/N_\text{DOF} < 10$
	Flight distance significance	$\chi^2_\text{FD} > 36$
$\overline{D}^0$	Mass	$1765 < m(h^+h^-h^+) < 1965\,\text{MeV}/c^2$
	Distance of closest approach	$\text{DOCA}(K^+, K^-) < 0.5\,\text{mm}$
	Direction angle	$\cos\theta > 0$
	Vertex quality	$\chi^2/N_\text{DOF} < 10$
	Flight distance significance	$\chi^2_\text{FD} > 36$
K^+ (π^+)	Track quality	$\chi^2/N_\text{DOF} < 4.0$
	Transverse momentum	$p_\text{T} > 100\,\text{MeV}/c$
	Momentum	$p > 1000\,\text{MeV}/c$
	Impact parameter significance	$\chi^2_\text{IP} > 4$
	Ghost track probability	$P_\text{Ghost} < 0.4$
	Particle identification	$\text{PIDK} < 20$ ($\text{PIDK} > -10$)

4.3.2 Particle identification requirements

Particle identification variables help to determine the species of tracks passing though the LHCb detector. Using information from the RICH sub-detectors, the likelihood of different mass hypotheses are compared to the pion hypothesis. Loose requirements are made on the kaon hypothesis PID variable to reduce the contribution from other types of hadrons and background from other b-hadron decays with misidentified hadrons.

4.3.3 Charmless and single-charm backgrounds

Decays of B^+ mesons that didn't proceed via a D meson could form a peaking background below the invariant mass distributions when they decay to the same final state. The signal mode could receive contributions from the decays $B^+ \to h^+h^-h^+\phi$ or $B^+ \to h^+h^-h^+h^+h^-$, referred to as charmless backgrounds. The normalisation mode is also susceptible, however as it involves two charm mesons it could receive contributions from the decays $B^+ \to h^+h^-h^+\overline{D}^0$ or $B^+ \to D_s^+h^+h^-$, referred to as single-charm backgrounds, and $B^+ \to h^+h^-h^+h^+h^-$ referred to as a charmless background. These backgrounds can be suppressed by requiring the D meson decay vertex to be displaced from the B^+ meson decay vertex. Requirements are applied to the significance of the vertex separation ($\chi^2_{\rm FD}$).

The residual yields of charmless backgrounds in the signal mode are estimated by performing a fit to the B^+ invariant mass for candidates with $25 < |m(h^+h^-h^+) - m(D_s^+)| < 50\,{\rm MeV}/c^2$. This background estimation is performed separately for the $B^+ \to D_s^+\phi$ and $B^+ \to D_s^+K^+K^-$ searches.

For the $B^+ \to D_s^+\overline{D}^0$ normalisation channel, a two-dimensional optimisation is performed to calculate the contribution from decays without a D_s^+ meson, $\overline{D}^0$ meson or both. The two-dimensional space defined by the D_s^+ and $\overline{D}^0$ masses is split into four types of area as shown in Fig 4.1:

1. Areas in which only $B^+ \to h^+h^-h^+h^+h^-$ decays contribute (red).

2. Areas in which either $B^+ \to D_s^+ h^+ h^-$ or $B^+ \to h^+ h^- h^+ h^+ h^-$ decays can contribute (blue).

3. Areas in which either $B^+ \to h^+ h^- h^+ \overline{D}^0$ or $B^+ \to h^+ h^- h^+ h^+ h^-$ decays can contribute (green).

4. The signal region in which $B^+ \to D_s^+ \overline{D}^0$, $B^+ \to h^+ h^- h^+ \overline{D}^0$, $B^+ \to D_s^+ h^+ h^-$ or $B^+ \to h^+ h^- h^+ h^+ h^-$ decays could contribute (black).

Asymmetric $\overline{D}^0$ sidebands are used to prevent misidentified $B^+ \to D_s^+ (\overline{D}^0 \to K^- \pi^+)$ decays from being included in the sideband sample. The optimal selection requirements are chosen such that the maximal signal efficiency is achieved for a residual charmless contribution of 2% of the normalisation yield.

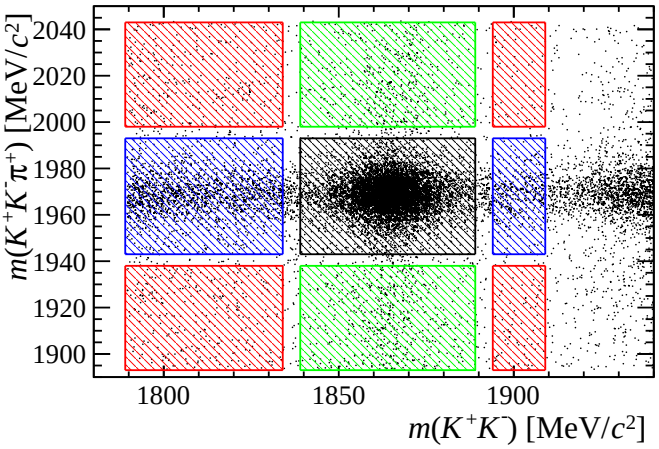

Figure 4.1: Two dimensional normalisation

- Include plots of selected cuts

4.3.4 Misidentified D and Λ_c^+ hadrons

It is possible for the samples D_s^+ mesons to be contaminated by other misidentified decays of D^+ mesons or Λ_c^+ baryons in which one of the decay products has been incorrectly identified. The invariant mass of the D_s^+ meson is recalculated, swapping the mass hypothesis of the ambiguous track to that of the K, or p, depending on

the decay mode. The particle identification requirements are tightened within a mass window around the D^+ or Λ_c^+ mass, effectively removing this crossfeed. For the mode $D_s^+ \to K^+K^-\pi^+$, the vetoes are not applied to candidates for which $m|(K^-K^+) - m_\phi| < 10\,\text{MeV}/c^2$ as there are a high purity of $D_s^+ \to K^+K^-\pi^+$ decays in this region.

The specific vetoes included in this selection are listed in Table 4.5.

Decay Mode	Misidentified decay
$D_s^+ \to K^+K^-\pi^+$	$D^+ \to \pi^+K^-\pi^+$
	$\Lambda_c^+ \to pK^-\pi^+$
$D_s^+ \to K^+\pi^-\pi^+$	$D^+ \to \pi^+\pi^-\pi^+$

Table 4.5: Misidentified decays targeted by vetoes. The ambiguous track is highlighted in red in each case.

The invariant mass distributions for each the misidentified $D_s^+ \to K^+K^-\pi^+$ decays are shown with and without the MVA requirements in Figs. 4.2 and 4.3 for both the signal $B^+ \to D_s^+\phi$ and normalisation $B^+ \to D_s^+\overline{D}^0$ decays.

- Include Descriptions
- Include plots of each applied

4.3.5 Invariant mass vetoes

Sharp peaking structures are observed in subsets of the final state particles. These are removed with simple invariant mass cuts to remove combinatorial or partially reconstructed backgrounds that result from these incorrectly reconstructed decays. For simplicity the final state particles for each mode are labelled with a number between 1–5 as described in Table 4.6.

All combinations of the final state particles that create a neutral or singly-charged candidate are investigated. Significant structures are observed for all three D_s^+ decay modes in some combination.

The following vetos are applied to remove these incorrectly reconstructed decays.

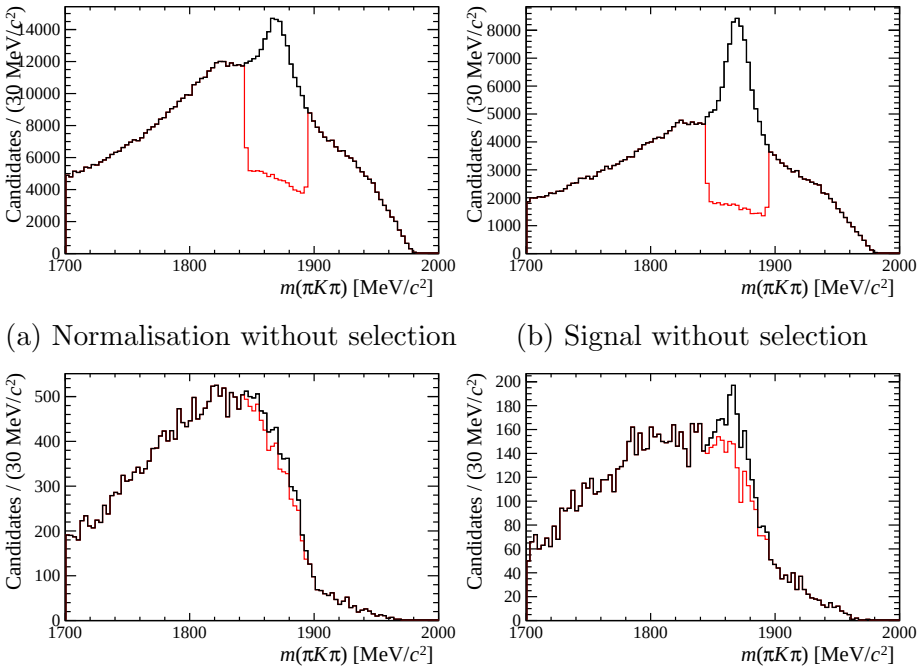

(a) Normalisation without selection (b) Signal without selection

(c) Normalisation with selection (d) Signal with selection

Figure 4.2: Invariant mass distributions of $D_s^+ \to K^+K^-\pi^+$ samples reconstructed as $D^+ \to \pi^+K^-\pi^+$ for the signal and normalisation samples. The samples are shown with (red) and without (black) the veto described in Sec. 4.3.4. The distributions are shown before (top) and after (bottom) the MVA requirements have been applied.

Decay Mode	1	2	3	4	5
$B^+ \to (D_s^+ \to K^+K^-\pi^+)\phi$	K^+	K^-	π^+	K^+	K^-
$B^+ \to (D_s^+ \to \pi^+\pi^-\pi^+)\phi$	π^+	π^-	π^+	K^+	K^-
$B^+ \to (D_s^+ \to K^+\pi^-\pi^+)\phi$	K^+	π^-	π^+	K^+	K^-

Table 4.6: Particle labels used when studying invariant mass vetoes.

- For the mode $B^+ \to (D_s^+ \to K^+K^-\pi^+)\phi$
  - $|m(1245) - m(B_s^0)| > 50\,\text{MeV}/c^2$
  - $|m(345) - m(D_s^+)| > 25\,\text{MeV}/c^2$ and $|m(345) - m(D^+)| > 25\,\text{MeV}/c^2$
- For the mode $B^+ \to (D_s^+ \to \pi^+\pi^-\pi^+)\phi$
  - $|m(145) - m(D_s^+)| > 25\,\text{MeV}/c^2$ and $|m(145) - m(D^+)| > 25\,\text{MeV}/c^2$
  - $|m(245) - m(D_s^+)| > 25\,\text{MeV}/c^2$ and $|m(245) - m(D^+)| > 25\,\text{MeV}/c^2$

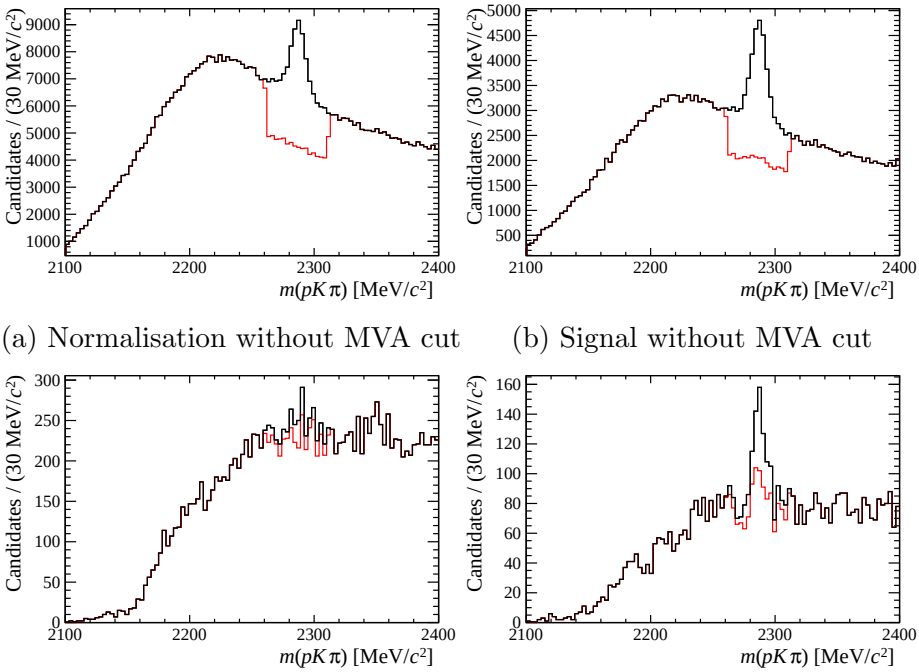

(a) Normalisation without MVA cut (b) Signal without MVA cut

(c) Normalisation with MVA cut (d) Signal with MVA cut

Figure 4.3: Invariant mass distributions of $D_s^+ \to K^+K^-\pi^+$ samples reconstructed as $\Lambda_c^+ \to pK^-\pi^+$ for the signal and normalisation samples. The samples are shown with (red) and without (black) the veto described in Sec. 4.3.4. The distributions are shown before (top) and after (bottom) the MVA requirements have been applied.

  - $|m(345) - m(D_s^+)| > 25\,\text{MeV}/c^2$ and $|m(345) - m(D^+)| > 25\,\text{MeV}/c^2$

- For the mode $B^+ \to (D_s^+ \to K^+\pi^-\pi^+)\phi$

  - $|m(245) - m(D_s^+)| > 25\,\text{MeV}/c^2$ and $|m(245) - m(D^+)| > 25\,\text{MeV}/c^2$
  - $|m(345) - m(D_s^+)| > 25\,\text{MeV}/c^2$ and $|m(345) - m(D^+)| > 25\,\text{MeV}/c^2$

In the search for $B^+ \to D_s^+K^+K^-$ decays the increased size of the $m(K^+K^-)$ phase space means more

4.3.6 Normalisation mode veto

In the search for $B^+ \to D_s^+K^+K^-$ decays, the phase space

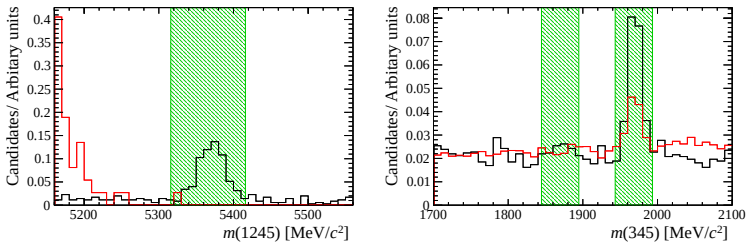

(a) $B^+ \to (D_s^+ \to K^+K^-\pi^+)\phi$

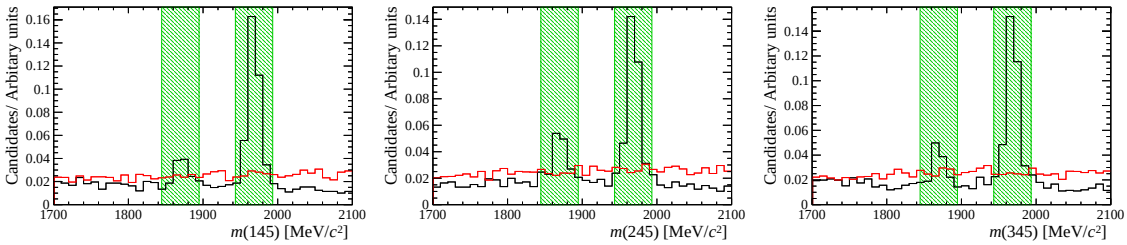

(b) $B^+ \to (D_s^+ \to \pi^+\pi^-\pi^+)\phi$

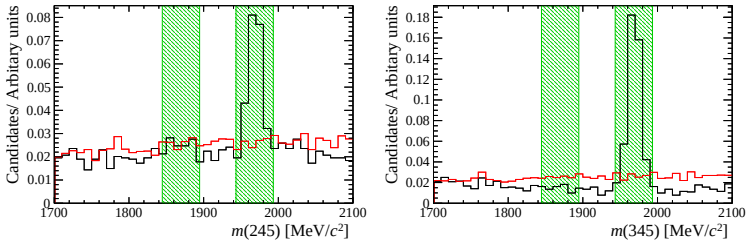

(c) $B^+ \to (D_s^+ \to K^+\pi^-\pi^+)\phi$

Figure 4.4: Invariant mass distributions for subsets of decay products. The green region show the regions removed by the vetoes listed in Sec 4.3.5.

4.3.7 Multivariate analysis

Multivariate Analyses (MVAs) are used to help discriminate between genuine D_s^+ and ϕ meson decays and random combinations of particles. These MVAs are trained using large samples of candidates from B mesons decays in data with similar topologies. This training can benefit from an expanded set of variables that are not perfectly represented in simulation, including tracking and PID information in addition to kinematic and geometric information. The distributions of the input variables are shown in Fig... The ϕ and D_s^+ MVAs use samples of $B_s^0 \to J/\psi\,\phi$ and $\overline{B}{}_s^0 \to D_s^+\pi^-$ decays, respectively. These are selected using dedicated Stripping Lines designed to select decays. To ensure these samples are representative of the target decays, a preselection is applied to the data. This comprises of similar trigger, background veto

and PID requirements applied to the signal modes. The ϕ and D_s^+ invariant mass distributions are fitted separately for each year.

where the background is statistically subtracted using the *sPlot* method [4]. The training uses the ϕ or D_s^+ sidebands as a background sample.

- Include plots example samples
- Include training variable distributions
- Comparison to alternative?

A total of eight MVAs are trained to target the decays $\phi \to K^+K^-$, $D_s^+ \to K^+K^-\pi^+$, $D_s^+ \to K^+\pi^-\pi^+$ and $D_s^+ \to \pi^+\pi^-\pi^+$, separately in the Run 1 (2011 and 2012) and Run 2 (2015 and 2016) data.

The samples are split into two random but reproducible subsamples. One is used to train the corresponding MVA, the other to test its response. The MVA method used in this analysis is a gradient Boosted Decision Tree (BDTG) [5]. The selection criteria for each of the BDTG classifiers are determined by optimising the Punzi figure of merit, $\epsilon_s/(\frac{a}{2} + \sqrt{N_{\rm BKG}})$ [6], with $a = 5$, where ϵ_s is the signal efficiency and $N_{\rm BKG}$ is the number of background candidates determined from fits to data, calculated in the signal region.

- Include plots of optimisation

The efficiencies of the MVAs are obtained from the testing samples of $B_s^0 \to J/\psi\,\phi$ and $B_s^0 \to D_s^+\pi^-$ decays. Additionally, a sample of $B^+ \to D^0\pi^+$ decays is used to calculate the efficiency of $\overline{D}^0 \to K^+K^-$ decays in the normalisation channel. The efficiency calculation takes into account the kinematic differences between the training and signal samples, as well as any possible correlations between the D_s^+ and ϕ kinematics, by using input from simulation samples. In the search for $B^+ \to D_s^+K^+K^-$ decays, calibration samples are used to correct for the imperfect modelling of the PID in simulation. These corrected simulations are then used to obtain the variations in the MVA efficiencies as a function of the phase-space position, in particular of the $m(K^+K^-)$ invariant mass.

4.4 Multiple candidates

4.5 Invariant mass distributions

- Include plots of D_s and K^+K^- mass after selection has been applied

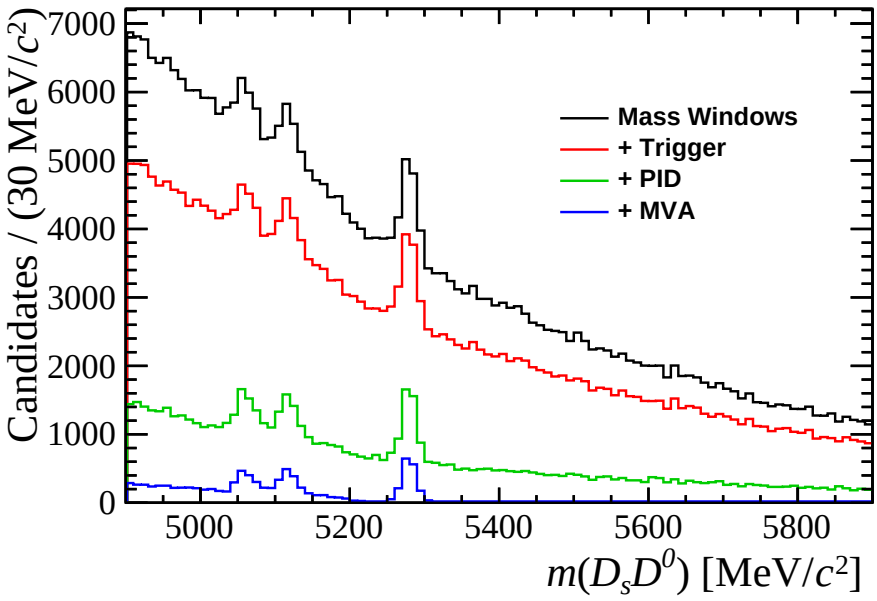

Figure 4.5: Various selection steps applied to the normalisation channel.

Chapter 5

Mass fit to $B^+ \to D_s^+ K^+ K^-$ candidates

Contents

In this chapter the methodology used to search for $B^+ \to D_s^+ K^+ K^-$ decays is described. The branching fraction $\mathcal{B}(B^+ \to D_s^+ K^+ K^-)$ is determined by measuring the ratio of $B^+ \to D_s^+ K^+ K^-$ and $B^+ \to D_s^+ \overline{D}^0$ yields. This is corrected by the ratio of efficiencies for the two modes and multiplied by the externally measured branching fractions for $B^+ \to D_s^+ \overline{D}^0$ and $\overline{D}^0 \to K^+ K^-$ decays.

$$\mathcal{B}(B^+ \to D_s^+ K^+ K^-) = \frac{N(B^+ \to D_s^+ K^+ K^-)}{N(B^+ \to D_s^+ \overline{D}^0)} \times \frac{\epsilon(B^+ \to D_s^+ \overline{D}^0)}{\epsilon(B^+ \to D_s^+ K^+ K^-)} \times \mathcal{B}(B^+ \to D_s^+ \overline{D}^0) \times \mathcal{B}(\overline{D}^0 \to K^+ K^-) \quad (5.1)$$

The fit models used to extract the yields $N(B^+ \to D_s^+ K^+ K^-)$ and $N(B^+ \to D_s^+ \overline{D}^0)$ are described in Section 5.1, the efficiency corrections are described in Section 5.5 and the resulting calculation of the branching fraction is in Section 5.7.

5.1 Fit components

In order to extract the yields of $B^+ \to D_s^+ \overline{D}^0$ and $B^+ \to D_s^+ K^+ K^-$ decays the invariant mass distributions for the processes contributing within the invariant mass range are parametrised with probability density functions (PDFs).

- mention fit range
- any other quantities that might be needed

5.1.1 Signal and normalisation decays

The invariant mass distribution of $B^+ \to D_s^+ \overline{D}^0$ and $B^+ \to D_s^+ K^+ K^-$ decays are parametrised as the sum of two Crystal Ball (CB) functions. The CB function consists of a Gaussian function with a power-law tail and is typically used to parametrise losses due to radiative processes. This is defined as

$$\mathrm{CB}(m, \mu, \sigma, n, \alpha) = \begin{cases} e^{-\frac{1}{2}\left(\frac{m-\mu}{\sigma}\right)^2}, & \text{if } \left(\frac{m-\mu}{\sigma}\right) < -|\alpha| \\ \frac{\left(\frac{n}{|\alpha|}\right)^n \times e^{-\frac{1}{2}|\alpha|^2}}{\left(\frac{n}{|\alpha|} - |\alpha| - \frac{m-\mu}{\sigma}\right)^n}, & \text{otherwise} \end{cases} \tag{5.2}$$

where μ, σ, n and α are adjustable parameters and m is the B meson invariant mass observable.

The sum of two CB functions is constructed with a variable fraction f_σ assigned to the CB function with the narrower width,

$$\mathrm{DCB}(m, \mu, \sigma_1, \sigma_2, n, \alpha) = f_\sigma \times \mathrm{CB}(m, \mu, \sigma_1, n, \alpha) + (1 - f_\sigma) \times \mathrm{CB}(m, \mu, \sigma_2, n, \alpha), \tag{5.3}$$

where the same tail parameters, n and α are used for both functions, but the widths, σ_1 and σ_2, are allowed to be different (with $\sigma_1 < \sigma_2$). As both CB shapes have

the same parameter α, the tails are constrained to be on the same side. Values for the adjustable parameters are determined from fits to simulated decays passing the selection requirements applied to the data. These are determined separately for the different D_s^+ decay modes. However, a number of parameters are not completely constrained from the simulations. The mean position μ is allowed vary freely in the fit to data, as is the narrowest CB width of the normalisation decay. The ratios σ_1/σ_2 and $\sigma_1(D_s^+\phi)/\sigma_1(D_s^+\overline{D}^0)$ are fixed from simulations. The tail parameters n and α are highly correlated, therefore the value of n is fixed to unity in both the fits to simulations and data.

Parameter	Value		
	$D_s^+ \to KK\pi$	$D_s^+ \to K\pi\pi$	$D_s^+ \to \pi\pi\pi$
$B^+ \to D_s\phi$			
σ_1/σ_2	0.49 ± 0.01	0.47 ± 0.01	0.46 ± 0.01
f_σ	0.80 ± 0.01	0.84 ± 0.01	0.81 ± 0.01
α	2.76 ± 0.07	3.06 ± 0.16	3.71 ± 0.23
n	1 ± 0	1 ± 0	1 ± 0
$B^+ \to D_s^+\overline{D}^0$			
σ_1/σ_2	0.43 ± 0.01	0.42 ± 0.01	0.40 ± 0.01
f_σ	0.88 ± 0.01	0.88 ± 0.01	0.88 ± 0.01
α	2.91 ± 0.06	3.36 ± 0.26	3.53 ± 0.25
n	1 ± 0	1 ± 0	1 ± 0
$\sigma_1(D_s^+\phi)/\sigma_1(D_s^+\overline{D}^0)$	1.27 ± 0.02	1.31 ± 0.02	1.26 ± 0.02

Table 5.1: Fixed values obtained in fits to MC used in the model for the signal pdf.

- plots of signal and normalisation fits

5.1.2 Partially reconstructed backgrounds

Partially reconstructed decays are those in which the five final state particles combined in the signal mode are only a subset of a background mode's final state. Decays of B mesons can contribute at lower invariant masses below the signal peak when one or more the decay products have not been reconstructed. For decays to contribute within the fitted B^+ invariant mass window, the particle or particles that have not

been reconstructed must be fairly low-momentum (soft) such that the invariant mass of the remaining particles is large.

Backgrounds to the normalisation channel

The low invariant mass region of the $D_s^+ \overline{D}^0$ spectrum is populated by decays of B^+ mesons to combinations of D and excited D mesons. These $\overline{D}^{*0}$ and D_s^{*+} mesons decay strongly to a ground state $\overline{D}^0$ or D_s^+ meson and a soft pion or photon. The branching fractions for these decays are listed in Table 5.2.

Decay	Branching fraction
$\overline{D}^{*0} \to \overline{D}^0 \gamma$	$(64.7 \pm 0.9)\%$
$\overline{D}^{*0} \to \overline{D}^0 \pi^0$	$(35.3 \pm 0.9)\%$
$D_s^{*+} \to D_s^+ \gamma$	$(93.5 \pm 0.7)\%$
$D_s^{*+} \to D_s^+ \pi^0$	$(5.8 \pm 0.7)\%$

Table 5.2: Branching fractions for excited charm mesons [3].

The excited charm mesons $\overline{D}^{*0}$ and D_s^{*+} (be more specific) are vector ($J^P = 1^-$) mesons. The partially reconstructed invariant mass of the D_s^+ and $\overline{D}^0$ mesons can vary depending on the spin of the missed particle. analytical PDFs are used to account for the spin of the missed particle. These were developed by considering the

- add formulas for hills and horns

Backgrounds to the signal channel

- plots of part reco shapes

5.1.3 Combinatorial background

The dominant source of background under the signal peak is due to combinations of unrelated tracks. This combinatorial background is modelled using an exponential function with a single degree of freedom controlling the effective slope of the shape.

- check what happens to the slopes

This slope is shared between the normalisation and signal channels, and between different D_s^+ decay modes. This adds stability to the fit.

5.2 Fit strategy

- Single fit to signal and normalisation
- $m(K^+K^-)$ range that goes into fit
-

5.3 Fit validation

- Toys for signal and normalisation
- why it doesnt matter that norm yield have wrong pulls
-

5.4 Normalisation and signal fits

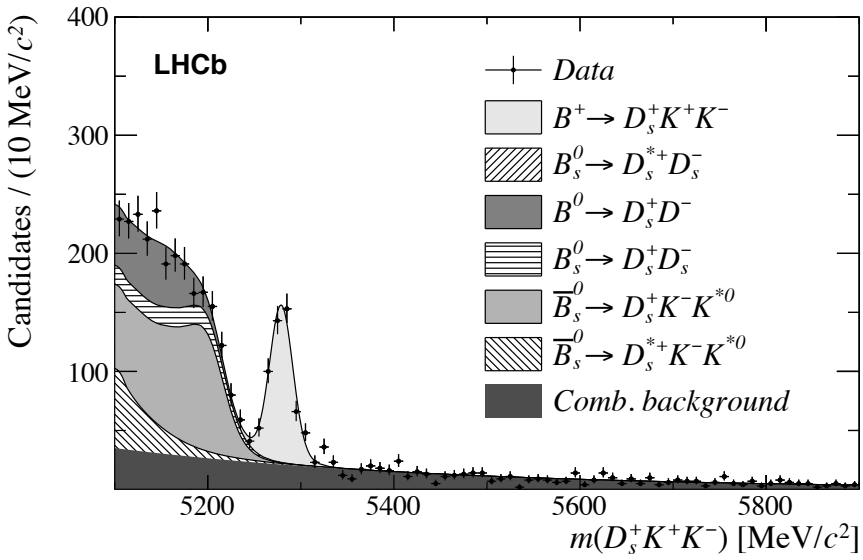

Figure 5.1: Invariant mass fit to $B^+ \to D_s^+ K^+ K^-$ candidates.

5.5 Efficiency corrections

- plots of eff accross dalitz plot
- studies of BDT eff ratio

5.6 Systematic uncertainties

5.7 Results

- Copy most of results section from paper
- equations
- include sWeighted, eff corrected plots
- include dalitz plot

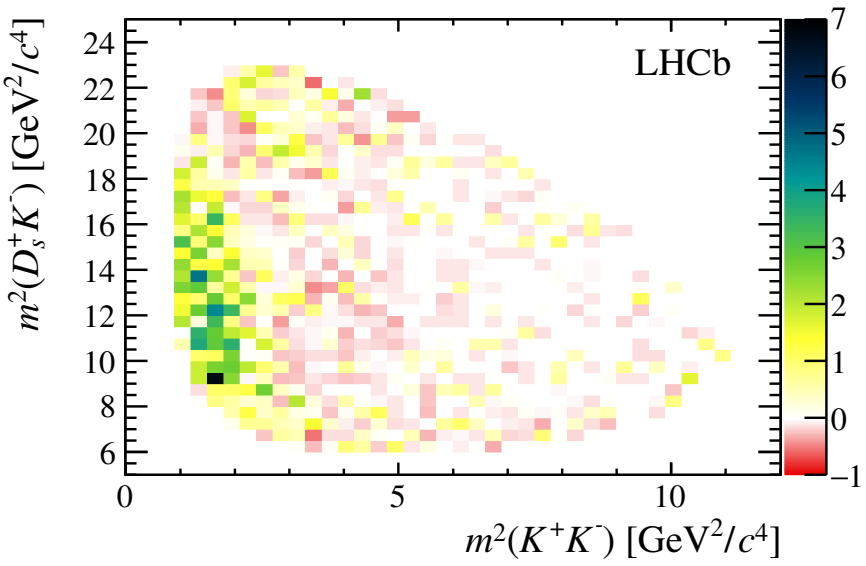

Figure 5.2: Dalitz plot

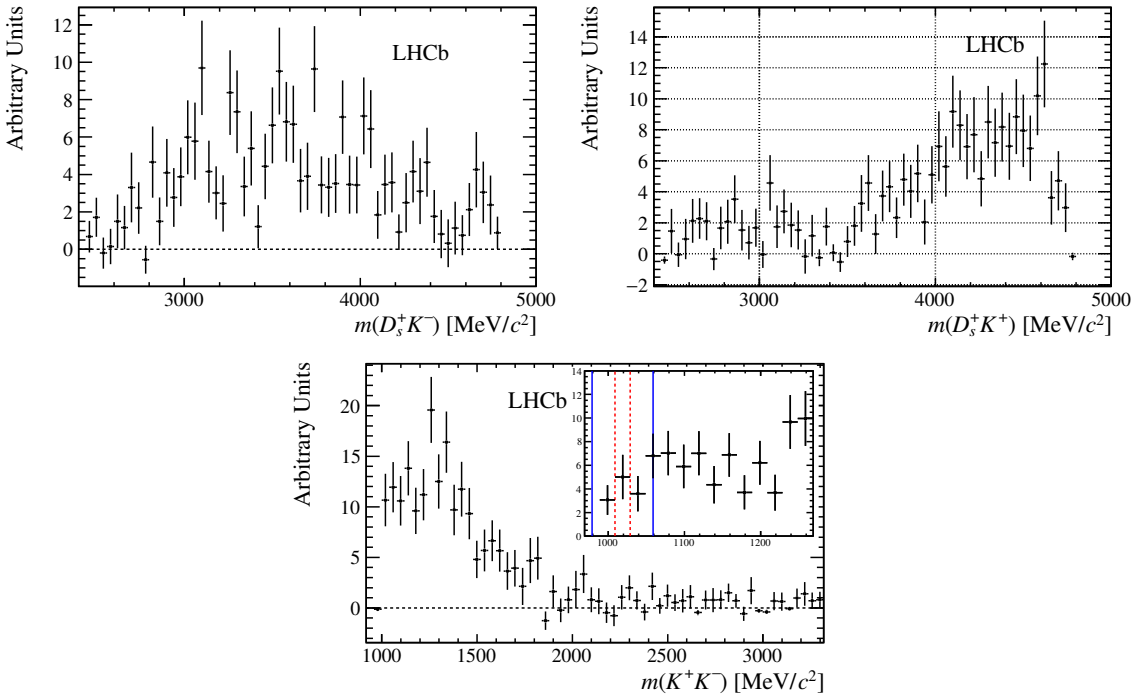

Figure 5.3: Two-body mass projections

Chapter 6

Mass fit to $B^+ \to D_s^+ \phi$ candidates

Contents

In this chapter the methodology used to search for $B^+ \to D_s^+ \phi$ decays is described.

- Details of blinding procedure for historic context

6.1 Fit components

6.1.1 Signal decays

- plots of signal shapes

6.1.2 Partially reconstructed backgrounds

- plots of partreco shapes

6.1.3 Combinatorial backgrounds

6.2 Fit strategy

The yield of $B^+ \to D_s^+ \phi$ candidates are determined using a simultaneous unbinned maximum likelihood fit in a number of different categories. These categories are designed to help separate the different contributions such that the relative contributions can be distinguished.

6.2.1 Simultaneous categories

- D_s^+ decay mode categories
- $m(K^+K^-)$ invariant mass categories
- helicity angle categories
- MC plots of each

6.2.2 $B^+ \to D_s^+ K^+ K^-$ model assumptions

- Studies with Laura++
- distributions of a number of models
- refer to $D_s^+ K^+ K^-$ plot
- final fraction

6.2.3 Fit validation

- Toy distributions

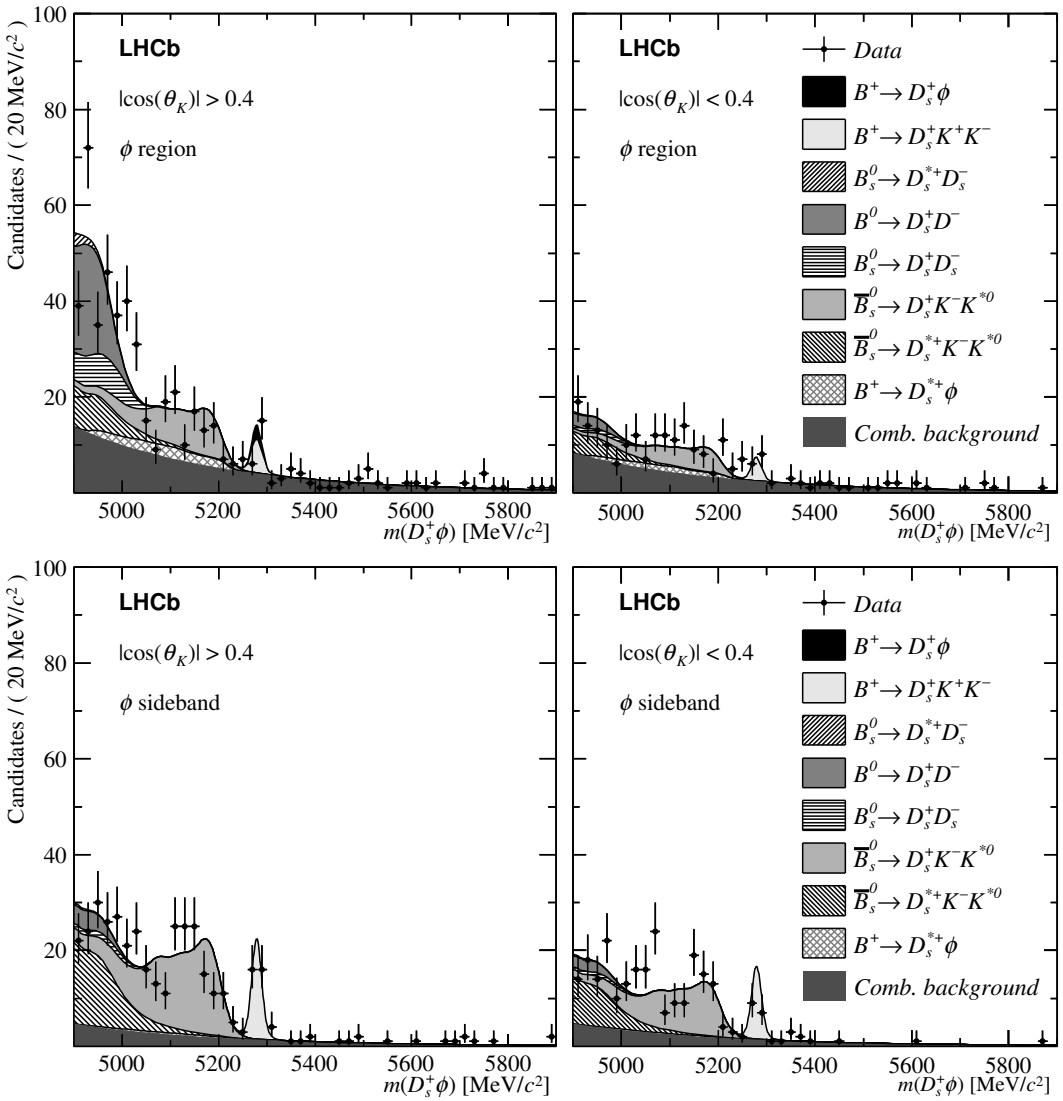

Figure 6.1: Invariant mass fits to $B^+ \to D_s^+ K^+ K^-$ candidates

6.3 Normalisation and signal fits

6.4 Efficiency corrections

- Assume pseudo two body decay, therefore simple ratio

6.5 Systematic uncertainties

6.6 Results

- Copy most of results section from paper

6.6.1 Limit setting

- Document all methods attemped
- CLs plots
- likelihood
- FC bands
- Table of comparison

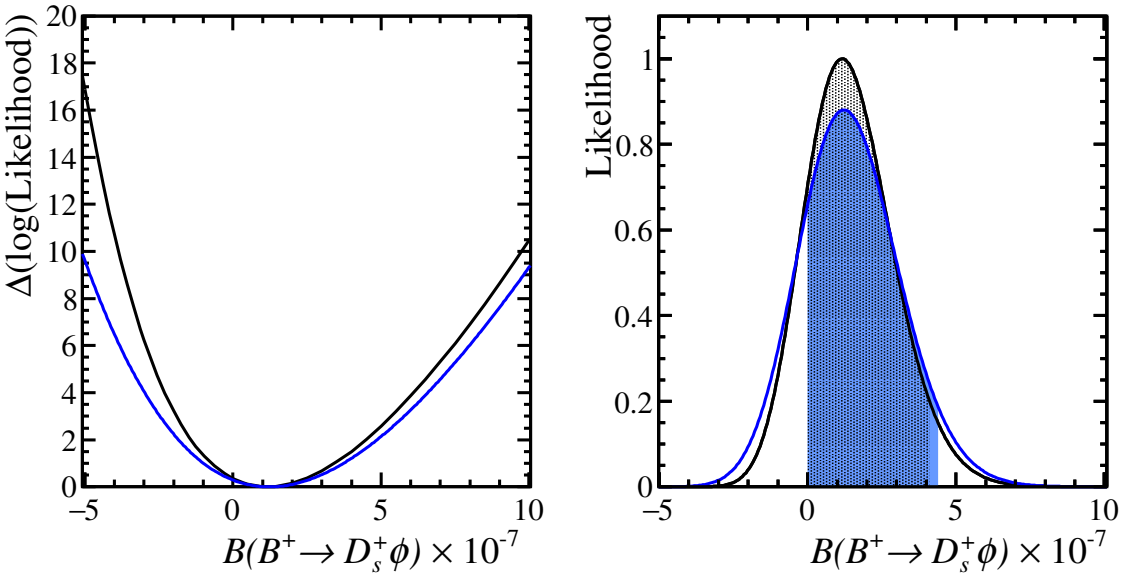

Figure 6.2: Bayesian profile likelihood limit determination

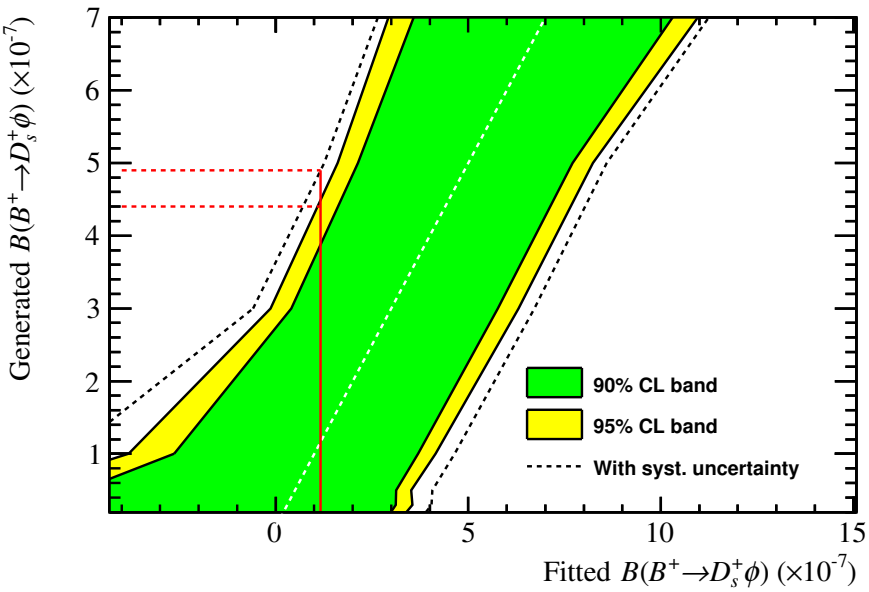

Figure 6.3: CLs limit determination

Bibliography

[1] LHCb collaboration, R. Aaij *et al.*, *A search for $B^+ \to D_s^+ K^+ K^-$ decays*, LHCb-PAPER-2017-032, in preparation.

[2] V. V. Gligorov and M. Williams, *Efficient, reliable and fast high-level triggering using a bonsai boosted decision tree*, JINST **8** (2013) P02013, arXiv:1210.6861.

[3] Particle Data Group, C. Patrignani *et al.*, *Review of particle physics*, Chin. Phys. **C40** (2016) 100001.

[4] M. Pivk and F. R. Le Diberder, *sPlot: A statistical tool to unfold data distributions*, Nucl. Instrum. Meth. **A555** (2005) 356, arXiv:physics/0402083.

[5] L. Breiman, J. H. Friedman, R. A. Olshen, and C. J. Stone, *Classification and regression trees*, Wadsworth international group, Belmont, California, USA, 1984.

[6] G. Punzi, *Sensitivity of searches for new signals and its optimization*, in *Statistical Problems in Particle Physics, Astrophysics, and Cosmology* (L. Lyons, R. Mount, and R. Reitmeyer, eds.), p. 79, 2003. arXiv:physics/0308063.